Deformation mechanisms leading to auxetic behaviour in the α-cristobalite and α-quartz structures of both silica and germania

2009 J. Phys.: Condens. Matter 21 025401

(http://iopscience.iop.org/0953-8984/21/2/025401)

IOP PUBLISHING JOURNAL OF PHYSICS: CONDENSED MATTER

J. Phys.: Condens. Matter **21** (2009) 025401 (12pp) doi:10.1088/0953-8984/21/2/025401

Deformation mechanisms leading to auxetic behaviour in the α-cristobalite and α-quartz structures of both silica and germania

A Alderson[1,3] **and K E Evans**[2]

[1] Centre for Materials Research and Innovation, University of Bolton, Deane Road, Bolton BL3 5AB, UK
[2] Advanced Technologies Research Institute, School of Engineering, Computing and Mathematics, University of Exeter, North Park Road, Exeter EX4 4QF, UK

E-mail: A.Alderson@bolton.ac.uk

Received 3 June 2008, in final form 2 September 2008
Published 9 December 2008
Online at stacks.iop.org/JPhysCM/21/025401

Abstract
Analytical expressions have been developed in which the elastic behaviour of the α-quartz and α-cristobalite molecular tetrahedral frameworks of both silica and germania are modelled by rotation, or dilation or concurrent rotation and dilation of the tetrahedra. Rotation and dilation of the tetrahedra both produce negative Poisson's ratios (auxetic behaviour), whereas both positive and negative values are possible when these mechanisms act concurrently. Concurrent rotation and dilation of the tetrahedra reproduces with remarkable accuracy both the positive and negative ν_{31} Poisson's ratios observed for silica α-quartz and α-cristobalite, respectively, when loaded in the x_3 direction. A parametric fit of the concurrent model to the germania α-quartz experimental ν_{31} Poisson's ratio is used to predict ν_{31} for germania α-cristobalite, for which no experimental value exists. This is predicted to be $+0.007$. Strain-dependent ν_{31} trends, due to concurrent rotation and dilation in the silica structures, are in broad agreement with those predicted from pair-potential calculations, although significant differences do occur in the absolute values. With the model of concurrent dilation and rotation of the tetrahedra we predict that an alternative uniaxial stress (σ_3)-induced phase exists for both silica, α-quartz and α-cristobalite, and germania, α-cristobalite, having geometries in reasonable agreement with β-quartz and idealized β-cristobalite, respectively.

1. Introduction

There is currently a great deal of interest in the development of 'negative' materials with counter-intuitive properties such as negative thermal expansion [1], negative permeability [2], negative permittivity [2], negative refractive index [3] and negative Poisson's ratios [4]. These unusual properties are related in some manner to the structural geometry of the materials, leading to a need to develop increased understanding of the mechanisms acting within the material nano-, micro- or macro-structures.

Negative Poisson's ratio materials undergo lateral expansion upon longitudinal tensile loading, and also lateral contraction under longitudinal compression. There is increasing interest in the development of these novel materials, known as *auxetic* materials [5], due to their counter-intuitive behaviour and also in applications where the auxetic property itself [4, 6], or enhancements in other materials properties due to a negative Poisson's ratio [4, 7], may be exploited. Enhanced indentation resistance [7] and fracture toughness [4] are among the properties that have been demonstrated to benefit from having a negative value of Poisson's ratio. Man-made and natural auxetic materials and structures exist from the molecular [6, 8] to the micro- [7, 9] and macroscopic levels [4, 10]. The

[3] Author to whom any correspondence should be addressed.

development of molecular auxetics [5, 11–13] is expected to lead to high modulus auxetic materials as well as having potential in sensor, molecular sieve and separation technologies [14, 15].

The discovery of auxetic behaviour at the molecular level in the α-cristobalite polymorph of crystalline silica [8] has led to an increase in research into the modelling, design and development of molecular auxetic materials [12, 13, 16–20]. Computer modelling calculations, based on classical interatomic potentials and on fully quantum-mechanical *ab initio* pseudopotentials, have previously been performed to investigate the elastic behaviour of both α-quartz and α-cristobalite [16–19]. A comprehensive study of the anisotropy of the Poisson's ratio in these polymorphs of silica is presented in [17]. The computer calculations are in reasonable agreement with the experimental Poisson's ratios for both polymorphs. It is difficult, however, to pinpoint the origin of the auxetic effect from computer calculations alone, since many different deformation mechanisms may be operating at a molecular level. One mechanism that has been suggested is the cooperative rotation of the SiO_4 tetrahedra leading to auxetic behaviour in α-cristobalite [8, 16, 17].

Rotation of rigid SiO_4 tetrahedra has been previously used as a model for lattice parameter changes in silica structures undergoing phase transitions or thermal expansion [21] and, more recently, in the 'rigid unit modes' (RUM) model for framework aluminosilicate crystals [22]. In the RUM model a certain number of phonon modes are considered to propagate through rotation and displacement of rigid SiO_4 and AlO_4 tetrahedra. Examples of RUMs known in silicates include those that alter the Si–O–Si bond angle and those that alter the O–O–O angle. RUMs can become energetically favourable due to the fact that the energy required to rotate linked tetrahedra about a common vertex is much less than that required to distort the tetrahedra through stretching of the strong Si–O bond. RUMs have been found to be important for a number of phenomena in tetrahedral framework structures, including providing the instability associated with structural phase transitions in quartz and cristobalite, and the effects of both tetrahedral stiffness and chemical composition on the phase transition temperature. Consequently, we expect the rotation of rigid tetrahedra to be worthy of consideration in the deformation response of quartz and cristobalite subject to uniaxial loading, and also for the investigation of the effect of the change in chemical composition from the silica to germania analogues.

We have recently shown that dilation of the tetrahedra (i.e. variation in tetrahedron size) can also lead to auxetic behaviour in the tetrahedral framework structure for α-cristobalite, and that both auxetic and non-auxetic behaviour are possible when rotation and dilation of the tetrahedra act concurrently [23]. Positive Poisson's ratios may be realized when one of the mechanisms acts to expand the structure while the other acts to contract the structure. This criterion may be satisfied when intertetrahedral and intratetrahedral forces within molecular tetrahedral framework structures are taken into account. Deformation due to simultaneous rotation and dilation of the tetrahedra has previously been considered in an attempt to understand the thermal expansion coefficients of crystal structures with tilts [24].

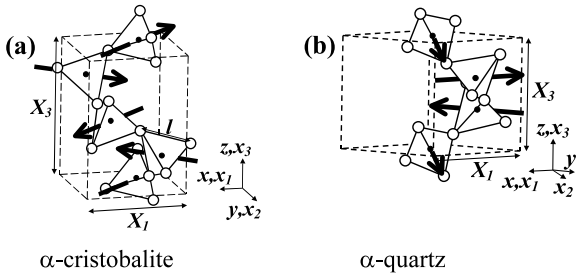

Figure 1. Tetrahedral framework unit cells for α-cristobalite and α-quartz showing tetrahedron rotation axes (solid arrows) and geometrical parameters. Filled circles are silicon atoms; empty circles are oxygen atoms.

We have now extended the models developed earlier [23] to include the related α-quartz structure, and have shown how they explain the dichotomy between auxetic and non-auxetic behaviour in the two silica polymorphs [25]. Here we report the full methodology employed in the development of the model for the α-quartz structure, compare this with the previous model for α-cristobalite and explain how auxetic and non-auxetic behaviour can be produced in both cases. This approach is then applied to germania. Experimental elastic constants for GeO_2 α-quartz are available for comparison [26]. We are unaware of any experimental elastic constants data available for GeO_2 α-cristobalite, and so we make a prediction of the Poisson's ratio for this system based on the parametric fit of the model to the quartz system.

Model predictions are also presented for the strain dependence of the Poisson's ratios and the existence of an interesting martensitic-like phase transition induced by a uniaxial stress, leading to predicted structures akin to those of β-quartz and β-cristobalite.

2. Tetrahedral framework structures

The basic molecular 'building block' for both the α-cristobalite and α-quartz polymorphs of crystalline silica is the nearly regular SiO_4 tetrahedron consisting of an O atom at each of the four corners surrounding a central Si atom. Both structures consist of a framework of corner-sharing SiO_4 tetrahedra in which each O atom is shared between two adjacent tetrahedra. α-cristobalite contains 4 tetrahedra per tetragonal primitive unit cell (space group $P4_12_12$) and α-quartz contains 3 tetrahedra per trigonal primitive unit cell (space group $P3_121$)—see figure 1. The germania polymorphs have essentially the same geometry, with silicon replaced by germanium.

Assuming regular tetrahedra of uniform size, then the lattice parameters for both α-cristobalite and α-quartz structures can be derived in terms of the tilt angle (δ) of a tetrahedron and the edge length (l) of a tetrahedron—see figures 1 and 2. δ is defined with respect to an axis passing through the midpoints of two opposing edges of each tetrahedron. For example in figure 2(a) the relevant tilt axis

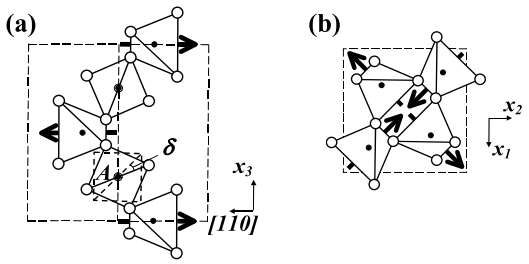

Figure 2. (a) x_3-[110] projection of the unit cell for α-cristobalite, showing tetrahedron axes and 'untilted' tetrahedron (A) to define tilt angle δ. (b) x_1–x_2 projection of the unit cell for α-cristobalite.

for tetrahedron A is out of the plane of the paper. The untilted ($\delta = 0$) orientation of tetrahedron A (indicated by a dashed outline) is shown with respect to the tilted tetrahedron (solid outline), clearly defining the angle of tilt, δ. We denote the mutually orthogonal principal axes as x_1, x_2 and x_3 and the crystallographic symmetry axes as x, y and z. The two sets of axes coincide for α-cristobalite. For α-quartz the x_1 and x_3 principal axes coincide with the x and z symmetry axes, respectively, and the y symmetry axis lies in the plane of the x_1 and x_2 principal axes but at an angle of 120° from the x_1 axis—see figure 1. For α-cristobalite the tilt axes are aligned parallel to the diagonals in the x–y plane; whereas they are parallel to either of the x or y axes or parallel to the short diagonal in the x–y plane for α-quartz. $\delta = 0$ when the top and bottom edges of each tetrahedron are perpendicular to the z axis—see, for example, the untilted ($\delta = 0$) tetrahedron A (dashed outline) in figure 2(a) for the α-cristobalite structure. Rotation of a tetrahedron corresponds to a variation in δ, whereas dilation of a tetrahedron corresponds to a variation in l.

In the case of α-quartz it is convenient to define a non-primitive unit cell with cell edges along the principal axes. The lattice parameters in the principal axis system are related to l and δ by:

$$X_1 = \frac{l(1+\sqrt{3}\cos\delta)}{\sqrt{2}} \tag{1}$$

$$X_2 = \sqrt{3}X_1 = \frac{\sqrt{3}l(1+\sqrt{3}\cos\delta)}{\sqrt{2}} \tag{2}$$

$$X_3 = \frac{3l\cos\delta}{\sqrt{2}} \tag{3}$$

where X_1, X_2 and X_3 are the lattice parameters in the x_1, x_2 and x_3 directions, respectively.

For α-cristobalite the lattice parameters are

$$X_1 = X_2 = l(1+\cos\delta) \tag{4}$$

$$X_3 = 2\sqrt{2}l\cos\delta. \tag{5}$$

3. Models

The Poisson's ratio ν_{ij} of a material under tension (or compression) in the x_i direction is defined by

$$\nu_{ij} = -\frac{\mathrm{d}\varepsilon_j}{\mathrm{d}\varepsilon_i} = -\frac{s_{ji}}{s_{ii}} \tag{6}$$

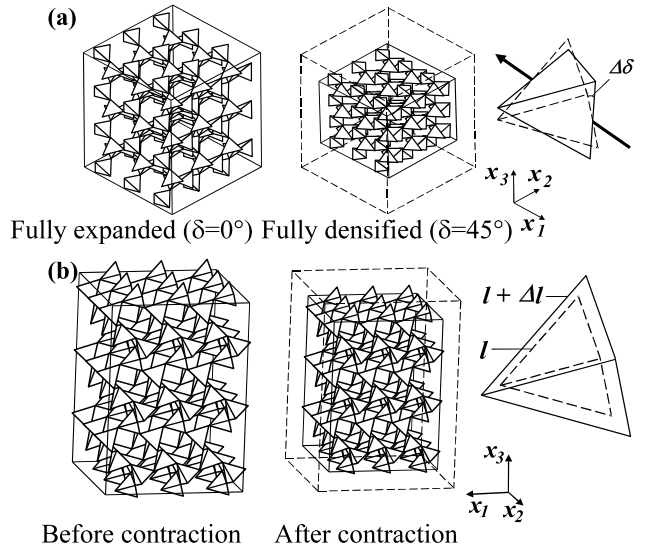

Figure 3. (a) Cooperative rotation of tetrahedra in which the tetrahedron size remains constant whereas the orientation of the tetrahedron varies during rotation. Fully expanded (i.e. $\delta = 0°$) and fully densified (i.e. $\delta = 45°$) $3 \times 3 \times 3$ extended tetrahedral networks are shown for α-cristobalite. (b) Dilation of tetrahedra in which tetrahedron size varies whilst the orientation of the tetrahedron remains constant during dilation. $3 \times 3 \times 3$ extended α-cristobalite tetrahedral networks are shown before and after contraction of the tetrahedra (δ = same value in both cases).

where $\mathrm{d}\varepsilon_i$ and $\mathrm{d}\varepsilon_j$ are the incremental true strains (and therefore are applicable to both linear and non-linear elastic deformation [27, 28]) in the mutually orthogonal x_i and x_j directions, respectively (i, $j = 1$, 2 or 3 and $i \neq j$) and the s's are elastic compliance coefficients (using conventional reduced matrix notation). Tensile strains are positive and contractile strains are negative. Hence a material in which longitudinal extension is accompanied by lateral expansion has a negative Poisson's ratio by virtue of having strains of equal sign.

We have previously developed three models for the deformation of the α-cristobalite structure in silica [23]. In the rotating tetrahedra model (RTM) deformation is assumed to be due to the cooperative rotation of rigid tetrahedra. The dilating tetrahedra model (DTM) assumes deformation occurs via size variation of a tetrahedron at fixed orientation. The third, concurrent tetrahedra model (CTM), assumes both rotation and dilation of a tetrahedron occur concurrently. From figure 3 it can be seen that both the RTM and DTM give rise to auxetic deformation. The CTM allows the possibility of both positive and negative Poisson's ratios to be realized when rotation and dilation of a tetrahedron act in an opposite sense to each other (i.e. one expands the structure whereas the other contracts the structure). This phenomenon is shown schematically in figures 4(a) and (b), and a more detailed discussion is given in [23], including the possibility of designing ultra-high Young's modulus materials.

The model expressions developed previously [23] for the α-cristobalite structure are quoted in table 1. In the following, equivalent expressions are derived for the α-quartz structure.

An infinitesimal incremental change of $\mathrm{d}X_i$ in the lattice parameter X_i corresponds to an infinitesimal increment of true

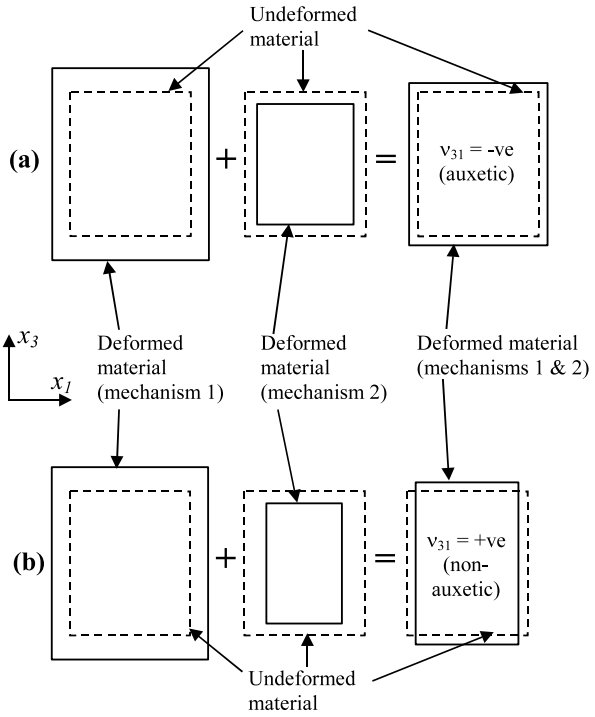

Figure 4. Schematic of a material deforming by two concurrent auxetic mechanisms (mechanisms 1 and 2) acting in opposite sense to each other (i.e. mechanism 1 expands the structure, mechanism 2 contracts the structure). (a) The lateral expansion due to mechanism 1 is greater than the lateral contraction due to mechanism 2, leading to overall auxetic behaviour. (b) The lateral expansion due to mechanism 1 is less than the lateral contraction due to mechanism 2, leading to overall non-auxetic behaviour.

strain in the x_i direction of

$$\mathrm{d}\varepsilon_i = \frac{\mathrm{d}X_i}{X_i} \tag{7}$$

where, for l and δ both varying

$$\mathrm{d}X_i = \frac{\partial X_i}{\partial \delta}\,\mathrm{d}\delta + \frac{\partial X_i}{\partial l}\,\mathrm{d}l. \tag{8}$$

Consider the changes in X_1, X_2 and X_3 due to rotation and dilation of a tetrahedron occurring simultaneously. Equations (1)–(3), (7) and (8) give

$$\mathrm{d}\varepsilon_1 = \mathrm{d}\varepsilon_2 = \frac{(1+\sqrt{3}\cos\delta)\,\mathrm{d}l - \sqrt{3}l\sin\delta\,\mathrm{d}\delta}{l(1+\sqrt{3}\cos\delta)} \tag{9}$$

and

$$\mathrm{d}\varepsilon_3 = \frac{(\cos\delta\,\mathrm{d}l - l\sin\delta\,\mathrm{d}\delta)}{l\cos\delta}. \tag{10}$$

Substituting equations (9) and (10) into (6) gives:

$$\nu_{12} = \nu_{21} = -1 \tag{11}$$

$$\nu_{31} = \nu_{13}^{-1} = -\frac{\sqrt{3}\cos\delta}{(1+\sqrt{3}\cos\delta)} \cdot \frac{\left(\frac{1}{\sqrt{3}} + \cos\delta - \kappa\sin\delta\right)}{(\cos\delta - \kappa\sin\delta)} \tag{12}$$

Table 1. RTM, DTM and CTM Poisson's ratio expressions derived for the tetrahedral frameworks of α-quartz and α-cristobalite.

Model	$\nu_{12} = \nu_{21}$	$\nu_{13} = \nu_{23} = \nu_{31}^{-1} = \nu_{32}^{-1}$
	α-cristobalite	
RTM	-1	$-\left(\frac{1+\cos\delta}{\cos\delta}\right)$
DTM	-1	-1
CTM	-1	$-\left(\frac{1+\cos\delta}{\cos\delta}\right)\left(\frac{\cos\delta-\kappa\sin\delta}{1+\cos\delta-\kappa\sin\delta}\right)$
	α-quartz	
RTM	-1	$-\left(\frac{1+\sqrt{3}\cos\delta}{\sqrt{3}\cos\delta}\right)$
DTM	-1	-1
CTM	-1	$-\left(\frac{1+\sqrt{3}\cos\delta}{\sqrt{3}\cos\delta}\right)\left(\frac{\cos\delta-\kappa\sin\delta}{\frac{1}{\sqrt{3}}+\cos\delta-\kappa\sin\delta}\right)$

where κ is a 'strength' parameter defined by

$$\kappa = l\frac{\mathrm{d}\delta}{\mathrm{d}l}. \tag{13}$$

Equations (11) and (12) give the analytical Poisson's ratios for the α-quartz structure of either silica or germania, assuming both rotation and dilation of a tetrahedron occur simultaneously, i.e. the CTM. The expressions for the RTM, in which deformation is by the cooperative rotation of rigid (constant l, i.e. $\mathrm{d}l = 0$) tetrahedra, are derived by substituting $\kappa = \infty$ in (12). Similarly, substituting $\kappa = 0$ into (12) yields the expression for the DTM, in which size variation of a tetrahedron occurs at fixed orientation ($\mathrm{d}\delta = 0$). Equation (11) is independent of κ, δ or l, with $\nu_{12} = -1$ for all 3 models. This corresponds to the structure maintaining transverse shape symmetry during deformation in each model.

4. Results

Table 2 summarizes the structural and mechanical property parameters determined experimentally and/or employed within the model calculations for the silica and germania analogues of α-quartz and α-cristobalite.

4.1. Positive and negative Poisson's ratios in the CTM

For both the quartz and cristobalite structures increasing δ leads to a decrease in the lattice parameters, whereas increasing l leads to an increase in the lattice parameters (see, for example, equations (1)–(5) and figure 3). Hence in the CTM both mechanisms act to expand (or contract) the structure for negative values of κ (i.e. $\mathrm{d}\delta$ and $\mathrm{d}l$ of opposite sign), leading to auxetic behaviour. Positive values of κ ($\mathrm{d}\delta$ and $\mathrm{d}l$ of the same sign) correspond to one of the mechanisms expanding the structure whereas the other contracts the structure. In this case an overall positive Poisson's ratio is possible when the Poisson's ratios associated with each deformation mechanism are different such that the overall longitudinal strain is tensile and the overall transverse strain is contractile for a longitudinal tensile load [23], see figure 4(b). From (12), positive values for

Table 2. Structural and mechanical properties employed in the calculations for silica and germania analogues of α-quartz and α-cristobalite.

	SiO_2		GeO_2	
	α-cristobalite	α-quartz	α-cristobalite	α-quartz
l (O–O) (Å)	2.63	2.63	2.85	2.85
θ (M–O–M) (deg)	146.4	144.4	128	130
R (M–O) (Å)	1.61	1.61	1.74	1.74
M . . . M (Å)	3.06	3.06	3.13	3.15
δ (deg)	23.5	16.3	34.0	26.5
ν_{12}	$+0.06 \pm 0.01$	$+0.141 \pm 0.002$		$+0.24$
ν_{13}	-0.10 ± 0.02	$+0.097 \pm 0.001$		$+0.21$
ν_{31}	-0.07 ± 0.01	$+0.127 \pm 0.001$		$+0.37$
$\mathrm{d}\sec\theta/\mathrm{d}R$ (Å^{-1})	-3.445	-3.445	-4.013	-4.013
κ	5.18 ± 0.07	5.18 ± 0.07	3.245	2.810

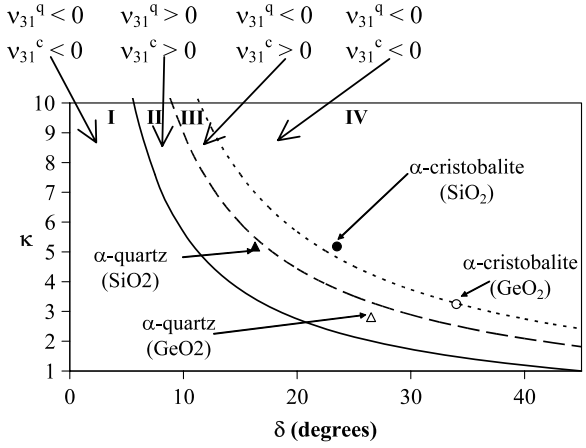

Figure 5. κ versus δ map for the CTM showing regions of positive and negative ν_{31} for the α-quartz ('α-q') and α-cristobalite ('α-c') structures. Region (I): ν_{31} negative for both structures; region (II): ν_{31} positive for both structures; region (III): ν_{31} negative for the α-quartz structure, positive for the α-cristobalite structure; region (IV): ν_{31} negative for both structures. Data points are shown for the predicted κ values and corresponding experimental values of δ for α-quartz (triangle) and α-cristobalite (circle) structures. Filled symbols correspond to SiO_2, empty symbols correspond to GeO_2.

ν_{31} are realized for the α-quartz structure when the following condition is satisfied:

$$\cot\delta < \kappa < \frac{\frac{1}{\sqrt{3}} + \cos\delta}{\sin\delta}. \tag{14}$$

Similarly, for the α-cristobalite structure ν_{31} is positive when [23]:

$$\cot\delta < \kappa < \frac{1 + \cos\delta}{\sin\delta}. \tag{15}$$

Regions of positive and negative ν_{31} are plotted on a κ versus δ map for the α-cristobalite and α-quartz structures in figure 5. There are four regions of behaviour corresponding to: (I) and (IV) ν_{31} is negative for both α-cristobalite and α-quartz; (II) ν_{31} is positive for both α-cristobalite and α-quartz; (III) ν_{31} is negative for α-quartz but positive for α-cristobalite. The boundaries of each region were calculated from equations (14) and (15).

4.2. Poisson's ratios of the undeformed silica and germania polymorphs

The experimental Poisson's ratios were calculated by employing the experimentally determined elastic compliance coefficients in (6) for silica α-cristobalite [8] and α-quartz [29], respectively. α-quartz has positive Poisson's ratios for uniaxial loading in all three principal directions ($\nu_{12} = \nu_{21} = +0.141 \pm 0.002$; $\nu_{13} = \nu_{23} = +0.097 \pm 0.001$; $\nu_{31} = \nu_{32} = +0.127 \pm 0.001$). α-cristobalite has both positive and negative principal Poisson's ratios ($\nu_{12} = \nu_{21} = +0.06 \pm 0.01$; $\nu_{13} = \nu_{23} = -0.10 \pm 0.02$; $\nu_{31} = \nu_{32} = -0.07 \pm 0.01$). Similarly, employing the experimentally determined elastic compliance coefficients in (6) for germania α-quartz [26], yielded the experimental Poisson's ratios for germania α-quartz. Germania α-quartz has positive Poisson's ratios for uniaxial loading in all three principal directions ($\nu_{12} = \nu_{21} = +0.24$; $\nu_{13} = \nu_{23} = +0.21$; $\nu_{31} = \nu_{32} = +0.37$). We have been unable to find any experimental data for germania α-cristobalite for comparison.

The calculated Poisson's ratios for α-cristobalite and α-quartz loaded along x_3 for all three analytical models are compared with experimental and computer modelling [16, 17, 26, 29, 30] data in table 3. The computer modelling calculations are in reasonable agreement with the experimental Poisson's ratios for both polymorphs. To test whether or not the rigidity of the SiO_4 tetrahedra contributed to the auxetic behaviour of α-cristobalite, pair-potential calculations have also previously been performed [16] with the O–O and Si–O bond distances constrained to remain fixed at the distances known to occur in crystals of these polymorphs. The Poisson's ratios (ν_{31}) thus calculated with this constraint of rigid SiO_4 tetrahedra are also included in table 3. The analytical model calculations employed the experimentally determined tilt angles of $\delta = 16.3°$ and 23.5° for silica α-quartz [31], and α-cristobalite [32], respectively and 26.5° and 34.0° for germania α-quartz [33], and α-cristobalite [34], respectively.

In considering the values of κ to be employed in the CTM for α-cristobalite and α-quartz it is instructive to expand the definition of κ given in (13) into the following form:

$$\kappa = l \cdot \frac{\mathrm{d}\delta}{\mathrm{d}\theta} \cdot \frac{\mathrm{d}\theta}{\mathrm{d}\sec\theta} \cdot \frac{\mathrm{d}\sec\theta}{\mathrm{d}R} \cdot \frac{\mathrm{d}R}{\mathrm{d}l}. \tag{16}$$

Table 3. ν_{31} Poisson's ratios for silica and germania α-quartz and α-cristobalite. Expt = experimental [8, 26, 29]; RTM = rotating tetrahedra model; DTM = dilating tetrahedra model; CTM = concurrent tetrahedra model; CM(ai) = computer modelling *ab initio* calculations [16, 17, 30]; CM(pp1) = computer modelling pair-potential calculations (constant strain method) [16, 17]; CM(pp2) = computer modelling pair-potential calculations (method of long waves) [17]; CM(rigid) = computer modelling pair-potential calculations (rigid SiO_4 tetrahedra constraint) [16, 17].

	SiO_2		GeO_2	
	α-quartz	α-cristobalite	α-quartz	α-cristobalite
Expt	$+0.127 \pm 0.001$	-0.07 ± 0.01	$+0.37$	
RTM	-0.62	-0.48	-0.61	-0.45
DTM	-1.00	-1.00	-1.00	-1.00
CTM	$+0.11 \pm 0.03$	-0.06 ± 0.01	$+0.370$	$+0.007$
CM(ai)	$+0.1$	-0.2	$+0.29$	
CM(pp1)	$+0.2$	-0.17		
CM(pp2)	$+0.19$	-0.05		
CM(rigid)	-0.6	-0.5		

In both polymorphs $l \sim 2.63$ Å (tetrahedron edge length = O–O bond length) for silica and 2.85 Å for germania. dR/dl is purely geometrical ($=\sqrt{3}/(2\sqrt{2})$; R = M–O bond length). $d\sec\theta/dR$ relates the amount of intertetrahedral angle change (θ = M–O–M angle) to the change in size of a tetrahedron and is related to the inter- and intratetrahedral forces. Both polymorphs contain tetrahedra of similar size (see above) and have similar intertetrahedral angles ($\theta \sim$ 144.4° and 146.4° for silica α-quartz [35] and silica α-cristobalite [36], respectively and 130° and 128° respectively for germania [33, 34]) and intertetrahedral distances (Si . . . Si distance ∼3.06 Å for the silica polymorphs [32, 33]; Ge . . . Ge distance ∼3.15 Å for the germania polymorphs [37]). Therefore, to a first approximation we expect the inter and intratetrahedral forces to yield similar values of $d\sec\theta/dR$ for both polymorphs if the CTM is valid. Hence it is reasonable to assume that, for a given chemical composition (SiO_2 or GeO_2), $l(d\sec\theta/dR)(dR/dl)$ will also be approximately equal for both polymorphs if the CTM is valid. $d\delta/d\theta$ and $d\theta/d\sec\theta$ are purely geometrical and expressions relating δ to θ have been derived elsewhere for α-quartz [31] and α-cristobalite [21] structures containing regular tetrahedra.

For the α-quartz structure:

$$\cos\theta = \tfrac{3}{4} - [\cos\delta + (2\sqrt{3})^{-1}]^2 \tag{17}$$

giving

$$\frac{d\delta}{d\theta} = -\frac{\sin\theta}{2[\cos\delta + (2\sqrt{3})^{-1}]\sin\delta}. \tag{18}$$

The expression for $d\theta/d\sec\theta$ is the standard differential:

$$\frac{d\theta}{d\sec\theta} = \frac{\cos^2\theta}{\sin\theta}. \tag{19}$$

Hence, from equations (17)–(19):

$$\frac{d\delta}{d\theta}\cdot\frac{d\theta}{d\sec\theta} = -\frac{\left\{\frac{3}{4} - [\cos\delta + (2\sqrt{3})^{-1}]^2\right\}^2}{2[\cos\delta + (2\sqrt{3})^{-1}]\sin\delta}. \tag{20}$$

For the α-cristobalite structure:

$$\cos\theta = \frac{(1 - 2\cos\delta - 2\cos^2\delta)}{3} \tag{21}$$

giving

$$\frac{d\delta}{d\theta} = -\frac{3\sin\theta}{2(1 + 2\cos\delta)\sin\delta}. \tag{22}$$

Equations (19), (21) and (22) yield:

$$\frac{d\delta}{d\theta}\cdot\frac{d\theta}{d\sec\theta} = -\frac{(1 - 2\cos\delta - 2\cos^2\delta)^2}{6[1 + 2\cos\delta]\sin\delta}. \tag{23}$$

From equations (20) and (23), and assuming that $l(d\sec\theta/dR)(dR/dl)$ is the same for both polymorphs, then the ratio of the strength parameters for α-quartz and α-cristobalite is dependent only on the respective values of δ:

$$\frac{\kappa_q}{\kappa_c} = \frac{\left\{\frac{3}{4} - [\cos\delta_q + (2\sqrt{3})^{-1}]^2\right\}^2}{[\cos\delta_q + (2\sqrt{3})^{-1}]\sin\delta_q} \times \frac{3(1 + 2\cos\delta_c)\sin\delta_c}{(1 - 2\cos\delta_c - 2\cos^2\delta_c)^2} \tag{24}$$

where the subscripts q and c refer to α-quartz and α-cristobalite, respectively. Employing the experimental values of $\delta_q = 16.3°$ and $\delta_c = 23.5°$ in (24) yields $\kappa_q/\kappa_c = 0.9995$ for the silica polymorphs.

We have shown elsewhere that if only bonded and next-nearest neighbour non-bonded interactions are considered then deformation resulting in a decrease in θ (contracting the structure, i.e. increasing δ—see equations (1)–(5)) may be accompanied by a concomitant increase in l (and R, i.e. expanding the structure) [23]. This, then, corresponds to a positive value of κ in the CTM. Molecular orbital calculations for α-quartz under thermal loading conditions show a linear relation between R and $-1/\cos\theta$ which implies l increases as θ decreases (δ increases) for $90° < \theta < 180°$ [31]. There is experimental evidence for such a relationship between the mean Si–O length and θ in both α-quartz and α-cristobalite (e.g. [32]), and also between the mean Ge–O length and θ in GeO_2 α-quartz [37]. Hence two deformation mechanisms acting in opposite senses to each other are known in these polymorphs. To a first approximation, then, we expect from simple geometrical considerations the strength parameters to be employed in the CTM for SiO_2 α-quartz and α-cristobalite to be positive and equal in magnitude if the CTM is valid.

Substituting the experimental values of ν_{31} and δ into the appropriate CTM expressions (table 1) yields $\kappa = 5.13$

and 5.24 for SiO_2 α-quartz and α-cristobalite, respectively. From the experimental errors associated with the ν_{31} and δ values we estimate uncertainties of around $\pm 2\%$ in κ for both polymorphs. The two values of κ thus obtained for α-quartz and α-cristobalite are, therefore, equal in magnitude (within error) and positive, providing excellent support for the validity of the CTM. The CTM ν_{31} values in table 3 for silica were, therefore, calculated using an average value of $\kappa = 5.18 \pm 0.07$ for both polymorphs. For both α-quartz and α-cristobalite the CTM ν_{31} values are in as good or better agreement with experiment than computer modelling calculations based on classical interatomic potentials and on fully quantum-mechanical *ab initio* pseudopotentials [16, 17].

From table 1 it is seen that all three analytical models predict $\nu_{12} = \nu_{21} = -1$ for both polymorphs. It is clear, therefore, that none of the analytical models are suitable for describing the deformation of these polymorphs when loaded in either of the transverse principal directions (x_1 or x_2) since the sign and magnitude of these Poisson's ratios are incorrectly predicted. Hence other models, possibly based on alternative tetrahedral rotation mechanisms and/or tetrahedral distortion effects, are likely to be required for deformation due to uniaxial transverse loading.

Substituting the experimental values of $\nu_{31} = +0.37$ and $\delta = 26.5°$ into the appropriate CTM expression (table 1) yields $\kappa = 2.81$ for GeO_2 α-quartz. Employing the experimentally determined tilt angles for the germania polymorphs ($\delta_q = 26.5°$ and $\delta_c = 34.0°$) in (24) yields $\kappa_q/\kappa_c = 0.8659$ for germania. Hence, assuming the CTM remains valid for loading along x_3 in the germania polymorphs, then a value of $\kappa = 3.245$ is calculated as the appropriate strength parameter for GeO_2 α-cristobalite. These values of κ were employed in the CTM calculations presented in table 3 for the GeO_2 polymorphs.

The calculated RTM ν_{31} values for the germania analogues show only a slight variation from those calculated for the silica counterparts even though the values of δ are significantly different. This is due to the fact that ν_{31} is largely insensitive to variations in δ for the RTM. Clearly the DTM calculations are the same for both the silica and germania polymorphs since $\nu_{31} = -1$ in all cases for the DTM. Interestingly, however, the CTM calculations predict that the germania α-cristobalite structure exhibits a very low (near zero) magnitude for ν_{31} and is non-auxetic ($\nu_{31} = +0.007$). This is opposite to the CTM-predicted and experimentally-observed values for silica α-cristobalite. The δ, κ coordinates for the germania and silica structures are also plotted on figure 5.

4.3. Strain-dependent ν_{31} variations

Strain-dependent variations in Poisson's ratio can be investigated by using the expanded form of $\mathrm{d}\delta/\mathrm{d}l$ given in (16) to derive an expression relating the change in tetrahedron edge length to the change in tilt angle at any value of δ. For example, from equations (13), (16) and (20), we find for α-quartz the following expression:

$$\mathrm{d}l = -\frac{4\sqrt{2}}{\sqrt{3}\left(\frac{\mathrm{d}\sec\theta}{\mathrm{d}R}\right)} \frac{\sin\delta[\cos\delta + (2\sqrt{3})^{-1}]}{\left\{\frac{3}{4} - [\cos\delta + (2\sqrt{3})^{-1}]^2\right\}^2}\mathrm{d}\delta. \quad (25)$$

Similarly, for α-cristobalite equations (13), (16) and (23) give

$$\mathrm{d}l = -\frac{6\sqrt{2}}{\sqrt{3}\left(\frac{\mathrm{d}\sec\theta}{\mathrm{d}R}\right)} \frac{\sin\delta\left(\frac{1}{2} + \cos\delta\right)}{\left(\frac{1}{2} - \cos\delta - \cos^2\delta\right)^2}\mathrm{d}\delta. \quad (26)$$

From equations (16), (20) and (23), a value of $\mathrm{d}\sec\theta/\mathrm{d}R = -3.445$ Å^{-1} is required to give $\kappa = +5.18$ for undeformed α-quartz and α-cristobalite ($\delta = 16.3°$ and 23.5°, respectively). Previous structural investigations indicate $\mathrm{d}\sec\theta/\mathrm{d}R$ remains approximately constant with deformation due to thermal [31, 32] and pressure [33, 38] loading. Hence, if $\mathrm{d}\sec\theta/\mathrm{d}R$ is assumed to also remain constant for deformation due to uniaxial loading of the structures along the x_3 direction, and the initial (i.e. undeformed) values of δ, κ and l are known, then equations (25) and (26) can be integrated and substituted into (16) to give the value of κ to be used in the appropriate CTM expression for ν_{31} (table 1) at any subsequent tilt angle during the deformation. For α-quartz we have

$$l = \frac{2\sqrt{2}}{\sqrt{3}\left(\frac{\mathrm{d}\sec\theta}{\mathrm{d}R}\right)\left\{\frac{3}{4} - [\cos\delta + (2\sqrt{3})^{-1}]^2\right\}} + \text{constant} \quad (27)$$

and for α-cristobalite

$$l = \frac{\sqrt{6}}{\left(\frac{\mathrm{d}\sec\theta}{\mathrm{d}R}\right)\left(\frac{1}{2} - \cos\delta - \cos^2\delta\right)} + \text{constant}. \quad (28)$$

The constants in equations (27) and (28) are found by substituting the initial values for l, δ and $(\mathrm{d}\sec\theta/\mathrm{d}R)$ into the expressions. The variation of ν_{31} with total true loading strain ε_3 is shown in figure 6(a) for both silica polymorphs. The total true strain in figure 6(a) was calculated by integrating (7) to give

$$\varepsilon_3 = \int_{X_{3(0)}}^{X_3} \frac{\mathrm{d}X_3}{X_3} = \ln\left(\frac{X_3}{X_{3(0)}}\right) \quad (29)$$

where X_3 and $X_{3(0)}$ are the deformed and undeformed lattice parameters along x_3 obtained by substituting the deformed and initial values, respectively, of l and δ in equations (3) and (5) for α-quartz and α-cristobalite. The deformed values of l were calculated from equations (27) and (28) for α-quartz and α-cristobalite, respectively. The CTM predicts ν_{31} for α-cristobalite will become positive under uniaxial compression and increasingly negative under tensile loading. For α-quartz ν_{31} is predicted to become increasingly positive under compression but is also predicted to be negative under sufficient tensile loading.

Strain-dependent Poisson's ratios have also been predicted from computer modelling calculations [16]. In [16] the Poisson's ratios were calculated from the ratio of total engineering strains (i.e. $-\varepsilon_1^{\mathrm{eng}}/\varepsilon_3^{\mathrm{eng}}$) whereas we have used the incremental true strain ratio (equation (6)) which is known to be appropriate for non-linear deformation [27, 28]. Hence to facilitate comparison between the two sets of data the computer modelling data have been converted into the incremental true strain ratio form used in this paper. The conversion was achieved by firstly calculating the engineering strain in the

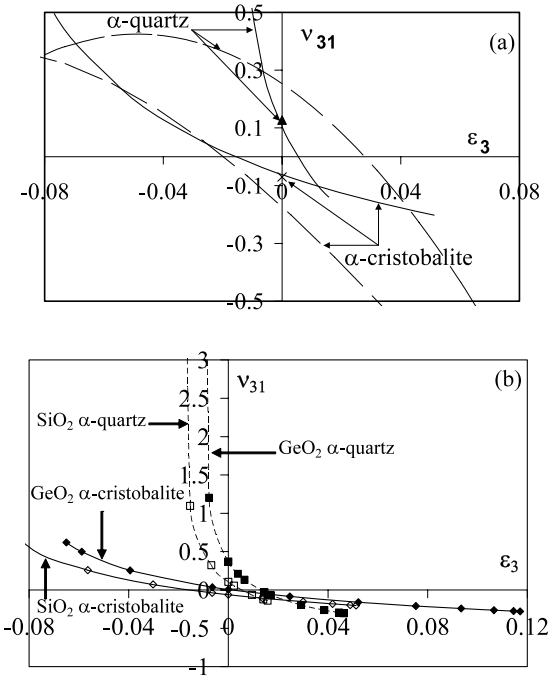

Figure 6. (a) ν_{31} versus ε_3 for SiO_2 α-quartz and α-cristobalite calculated from the CTM (solid curves) and pair-potential calculations [16] (dashed curves). Experimental data are also shown for undeformed α-quartz (triangle) [29] and α-cristobalite (cross) [8]. (b) ν_{31} versus ε_3 for GeO_2 (filled symbols) and SiO_2 (empty symbols) α-quartz and α-cristobalite calculated from the CTM. In the CTM calculations, undeformed values of $\delta = 16.3°$ and $\kappa = 5.18$ were used for SiO_2 α-quartz, $\delta = 23.5°$ and $\kappa = 5.18$ were used for SiO_2 α-cristobalite; $\delta = 26.5°$ and $\kappa = 2.810$ were used for GeO_2 α-quartz, and $\delta = 34.0°$ and $\kappa = 3.245$ were used for GeO_2 α-cristobalite.

x_1 direction ($\varepsilon_1^{\text{eng}}$) using $\varepsilon_1^{\text{eng}} = -\nu_{31}^{\text{eng}}\varepsilon_3^{\text{eng}}$ (where ν_{31}^{eng} is the Poisson's ratio calculated from the total engineering strain ratio, and ν_{31}^{eng} and $\varepsilon_3^{\text{eng}}$ are provided in [16]). Secondly, the total engineering strains were converted to total true strains using the standard conversion $\varepsilon_i = \ln(1+\varepsilon_i^{\text{eng}})$. Finally, strain-dependent ν_{31} values were calculated from the gradient of a plot of ε_1 versus ε_3 (i.e. the definition from (6)).

The converted computer modelling ν_{31} versus ε_3 data are also included in figure 6(a). The general trends from the computer modelling calculations are in agreement with those from the CTM (i.e. ν_{31} is positive under increased compression and negative under increased tension, with α-cristobalite and α-quartz being auxetic and non-auxetic, respectively, in the undeformed state). However, for both structures ν_{31} is predicted by the computer modelling calculations to reach a plateau under large compressive strain whereas it is predicted to continue to become increasingly positive in the CTM. The ν_{31} values are also predicted to reach more negative values in the computer modelling calculations than in the CTM.

The experimental data for undeformed α-cristobalite and α-quartz are also included in figure 6(a). The CTM calculations are in better agreement with the experimental data than the computer modelling calculations.

Using the same analytical method for germania, but with the appropriate data, $\delta = 26.5°$ and $34.0°$, and $\kappa = 2.810$ and 3.245 for undeformed GeO_2 α-quartz and GeO_2 α-cristobalite, generates the curves in figure 6(b) (filled symbols). The trends are similar to those predicted by the CTM for the silica counterparts (empty symbols in figure 6(b)), i.e. compression along x_3, causes an increasingly positive value for ν_{31}, whereas extension along x_3 leads to a reduction and eventual transition to negative value for ν_{31} for both polymorphs.

The strain magnitudes considered in the model predictions in figures 6(a) and (b) are of the order of a few per cent strain and are consistent with those used in the previous computer modelling simulations [16] and in temperature and pressure studies for both the germania and silica polymorphs [30–33, 35, 38].

4.4. Predicted σ_3-induced second phases in the cristobalite and quartz structures

We have previously shown that the CTM predicts a second stable phase exists for any given value of the strength parameter κ[21]. The strain energy per unit volume of a material, U, is derived from classical elasticity theory to be:

$$U = \tfrac{1}{2}\sigma_i\varepsilon_i = \tfrac{1}{2}E_i\varepsilon_i^2 \tag{30}$$

where σ_i and E_i are the stress and Young's modulus, respectively, in the x_i direction. We have seen from comparison with experimental ν_{12} and ν_{21} values that the CTM is not a valid model for α-cristobalite and α-quartz when loaded in the x_1 and x_2 directions (this is also confirmed by comparison of the model and experimental ν_{13} and ν_{23} values). Hence, we consider only the case of a uniaxial stress applied in the x_3 direction (σ_3) (i.e. $\sigma_1 = \sigma_2 = 0$ since the deformation mechanisms in the CTM do not operate in these loading cases). Therefore, for these structures, considering terms for uniaxial loading in the x_3 direction in (30) for the CTM, we can define a normalized strain energy function by

$$U^* = \frac{2U}{E_3} = \varepsilon_3^2. \tag{31}$$

Now, for a given value of κ we have from (13)

$$\int_{\delta_\alpha}^{\delta} \mathrm{d}\delta = \kappa \int_{l_\alpha}^{l} \frac{\mathrm{d}l}{l} \tag{32}$$

giving

$$l = l_\alpha \exp\left(\frac{\delta - \delta_\alpha}{\kappa}\right) \tag{33}$$

where l_α and δ_α are the tetrahedron edge length and tilt angle, respectively, for the α-phase, and the tilt angles are in radians. The normalized strain energy function for the quartz structure loaded in the x_3 direction is then derived from equations (3), (29), (31) and (33) to be:

$$U^*_{\text{CTM}} = \left[\left(\frac{\delta - \delta_\alpha}{\kappa}\right) + \ln\left(\frac{\cos\delta}{\cos\delta_\alpha}\right)\right]^2 \tag{34}$$

where $\delta_\alpha = 16.3°$ and the subscript 'CTM' indicates that the normalized strain energy function refers to the CTM. Equation (34) also holds for the cristobalite structure (with

$\delta_\alpha = 23.5°$). Note that, for a given value of κ, the normalized strain energy function depends only on the tilt angle of a tetrahedron, i.e. it is independent of l, the edge length of a tetrahedron.

Expressions for the RTM and DTM can also be derived. The normalized strain energy function for the RTM is derived by substituting $\kappa = \infty$ (i.e. $\mathrm{d}l = 0$ in (13)) in (34):

$$U^*_{\mathrm{RTM}} = \left[\ln\left(\frac{\cos\delta}{\cos\delta_\alpha}\right)\right]^2. \tag{35}$$

In the case of the DTM then equations (3), (5), (29) and (31) yield

$$U^*_{\mathrm{DTM}} = \left[\ln\left(\frac{l}{l_\alpha}\right)\right]^2 \tag{36}$$

for both structures.

Figures 7(a) and (b) show the normalized strain energy as a function of tilt angle for the silica quartz ($\delta_\alpha = 16.3°$) and silica cristobalite ($\delta_\alpha = 23.5°$) structures, respectively. In each case curves are calculated for the CTM, RTM and DTM, and δ_α corresponds to the value of the tilt angle known to occur in the α-phase. Stable phases are indicated by minima in the U^* versus δ curves. For the DTM only one minimum is predicted ($\delta = \delta_\alpha$), indicating that no other phase is predicted by the DTM. The RTM curves are symmetrical about $\delta = 0°$ and so two phases (minima) are predicted, corresponding to $\delta = \pm\delta_\alpha$. However, since the sign of the tilt angle of the tetrahedra is a purely arbitrary choice then the two phases predicted by the RTM will be energetically equivalent and indistinguishable from each other and so will both correspond to a degenerate α-phase. The CTM, on the other hand, predicts two distinct phases for both structures. For the quartz structure ($\delta_\alpha = 16.3°$) a σ_3-induced second silica phase is predicted by the CTM to occur at $\delta = 5.5°$ for $\kappa = 5.18$. For the cristobalite structure the CTM predicts the σ_3-induced second silica phase will occur when $\delta = -2.0°$ (for $\kappa = 5.18$ and $\delta_\alpha = 23.5°$). Employing these values for the second phases in the CTM expressions yields predicted values of $\nu_{31} = -1.4$ and -0.9 for quartz and cristobalite, respectively. In other words, the predicted σ_3-induced second phases are predicted by the CTM to be auxetic for both silica quartz and silica cristobalite.

Figure 7(c) shows the normalized strain energy as a function of tilt angle for GeO_2 quartz ($\delta_\alpha = 26.5°$) and GeO_2 cristobalite ($\delta_\alpha = 34.0°$) structures, respectively. Figure 7(c) shows that σ_3-induced second phases for the germania quartz and cristobalite structures are predicted by the CTM to occur at $\delta = 12.5°$ ($\kappa = 2.810$) and $-0.8°$ ($\kappa = 3.245$), respectively. By analogy with silica we know quartz and cristobalite each has two phases. Employing these values for the second phases in the CTM expressions yields predicted ν_{31} values of -1.6 and -1.0, respectively. Hence ν_{31} values for the second phases of the germania structures are predicted by the CTM to have opposite signs to those for the α phases.

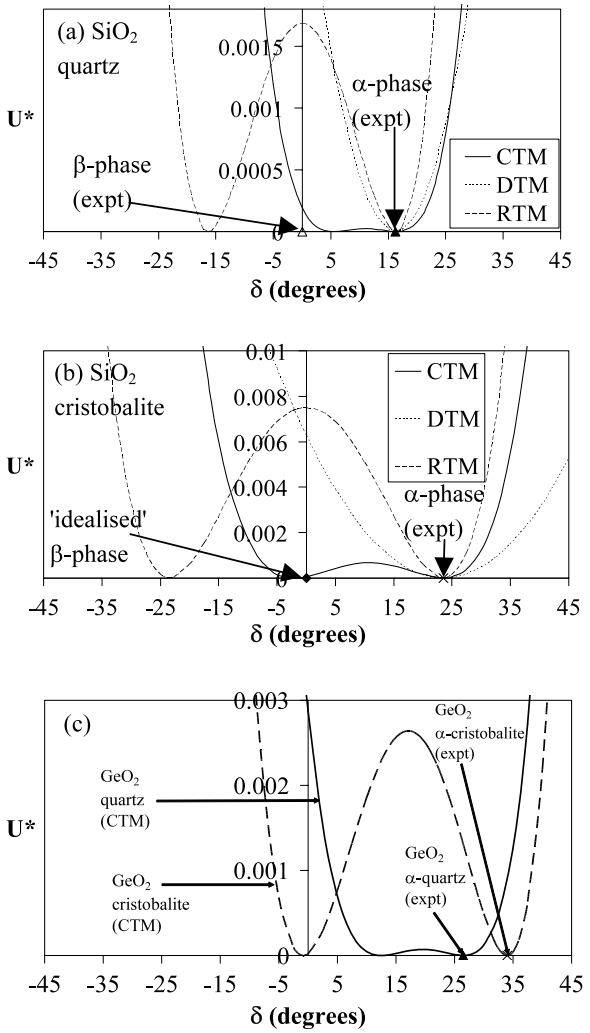

Figure 7. Normalized strain energy (U^*) versus tilt angle (δ) predictions from the DTM, RTM and CTM ($\kappa = 5.18$) for (a) SiO_2 quartz ($\delta_\alpha = 16.3°$) and (b) SiO_2 cristobalite ($\delta_\alpha = 23.5°$). (c) Normalized strain energy (U^*) versus tilt angle (δ) predictions from the CTM for GeO_2 quartz ($\delta_\alpha = 26.5°$, $\kappa = 2.810$—solid line) and GeO_2 cristobalite ($\delta_\alpha = 34.0°$, $\kappa = 3.245$—dashed line).

5. Discussion

5.1. Silica

Comparison of the CTM model calculations with experimental data shows excellent agreement, demonstrating that single-crystal silica α-quartz and silica α-cristobalite are examples of two molecular materials for which the model of concurrent rotation and dilation of a tetrahedron is valid for loading in the x_3 direction. α-cristobalite exhibits auxetic functionality as a result of two independent auxetic mechanisms acting concurrently. α-quartz, on the other hand, provides clear evidence that two auxetic deformation mechanisms can lead to non-auxetic behaviour when one (i.e. RTM) acts to expand the structure and the other (i.e. DTM) acts to contract it. The remarkable accuracy with which the values of the real materials are predicted by a model having only a few degrees of freedom indicates that tetrahedron distortion is not a significant deformation mechanism for loading along the x_3 direction. Force-field-based molecular modelling simulations have recently been performed for uniaxial loading along each principal direction of SiO_2 α-cristobalite [39]. The simulations indicate uniform variation of the intertetrahedral Si–O–Si angle (θ) for loading along the x_3 direction,

indicative of the cooperative rotation of tetrahedra mechanism considered here.

The CTM fails to accurately predict the Poisson's ratios of SiO_2 α-quartz and SiO_2 α-cristobalite for loading in either the x_1 or x_2 direction, possibly indicating the need to incorporate tetrahedron distortion and/or one or more additional rigid unit modes to accurately predict the micromechanical mechanisms for transverse uniaxial loading. The recent force-field-based simulations indicate that uniaxial loading along either of the x_1 or x_2 directions leads to a divergence of the intertetrahedral Si–O–Si angles into two distinct values and is consistent with an additional rigid unit mode comprising cooperative rotation of each tetrahedron about the tetrahedron axis most closely aligned along the x_3 axis [39, 40]. Similarly, divergent Si–O–Si (θ) angles would lead to divergent tilt angle (δ) values for the rigid unit rotation mode considered in the model presented in this paper (equations (17) and (21) for α-quartz and α-cristobalite, respectively). This would also lead to divergent edge length (l) values (equations (25) and (26)) and, therefore, an inevitable tendency for distortion of the tetrahedra.

Tetrahedral rotation is known to occur for hydrostatic pressure and thermal loading of SiO_2 α-quartz and SiO_2 α-cristobalite. However, it can be shown that a single value of κ employed within the CTM cannot accurately predict the strain response of both SiO_2 α-quartz and SiO_2 α-cristobalite under either of these conditions and so the CTM does not appear to be valid for pressure or thermal loading. It appears, then, that the necessary conditions for the two mechanisms employed in the CTM to be the predominant mechanisms in SiO_2 α-quartz and SiO_2 α-cristobalite correspond to the specific case of a uniaxial applied load along the x_3 direction. For this reason, the remainder of this paper has concentrated only on the Poisson's ratio for loading along x_3. We leave the development of a model containing the salient mechanisms for transverse uniaxial loading to a later paper.

The strain-dependent ν_{31} trends calculated from the CTM are consistent with those from computer modelling calculations for loading along x_3, i.e. at the largest compressive loads ν_{31} is positive whereas at the largest tensile loads ν_{31} is negative for both polymorphs (figure 6(a)). ν_{31} has also been predicted from pair-potential calculations to be negative for α-quartz under reduced hydrostatic pressure and is known to be negative at elevated temperatures (800–850 K) [41]. However, there are discrepancies between the CTM and computer modelling predictions at high tensile and compressive strains, probably due to a breakdown in the assumptions employed in the calculation of κ under extreme tension and compression.

The CTM predicts that a σ_3-induced second phase exists for both polymorphs. The β-quartz structure is known [31] to correspond to the 'untilted' geometry (i.e. $\delta = 0$), which is in reasonable agreement with that predicted by the CTM (figure 7(a)). There is not, however, a consensus in the literature on the actual structure of β-cristobalite. The 'idealized' structure originally proposed [42] for β-cristobalite, corresponding to the 'untilted' ($\delta = 0$) geometry, contains collinear Si–O–Si bonds (figure 8(b)) and requires an Si–O bond length of 1.54 Å in order to reproduce the volume change known to occur when undergoing the α-to-β phase transformation. Si–O–Si bond angles of 180° are unusual in silica polymorphs, and the required Si–O bond length is small compared to the typical value for silica of ∼1.61 Å. Consequently a locally ordered structure ('ordered' β-cristobalite) [21, 43, 44] has also been proposed. Ordered β-cristobalite is derived from the idealized β-cristobalite structure by rotation of each tetrahedron by an angle ϕ (=19.8°) about the tetrahedron axis aligned along the x_3 direction (figure 8(c)). The ordered structure requires the more realistic Si–O bond length of 1.61 Å to achieve the correct volume change associated with the α-to-β phase transformation. Note that both idealized and ordered β-cristobalite have $\delta = 0$. Yet other views proposed include that β-cristobalite has a dynamically disordered framework in which the oxygen atoms precess about the Si–Si axes in the idealized structure [45], and that the β-cristobalite structure is a dynamic average of domains of α-cristobalite [46].

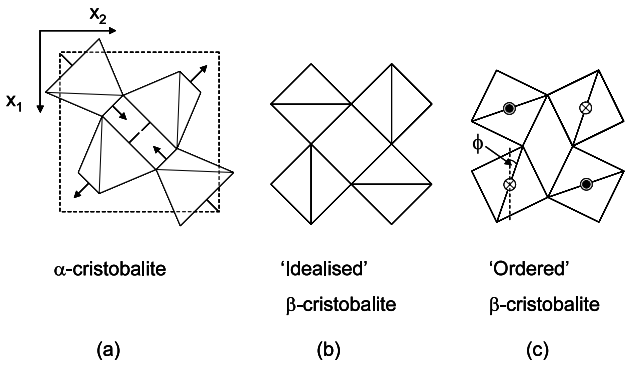

Figure 8. Projections in the x_1–x_2 plane of (a) α-cristobalite, (b) idealized β-cristobalite and (c) ordered β-cristobalite.

Using the CTM we propose that the 'ideal' structure for β-cristobalite has a tilt angle of $\delta \sim 0°$ (figure 7(b)). Both the predicted second phases occurring at $\delta \sim 0$ in the CTM are stabilized as a result of dilation/contraction of the tetrahedra (since the structures at $\delta = 0$ are predicted to be unstable in the RTM). Hence in addition to removing the tilt of the tetrahedra, we must also expect variation of the size of the tetrahedra to occur at the phase transition as implied by (33). In separate work we have shown that a σ_3-induced phase transition to ordered β-cristobalite can be modelled by force-field-based simulations [39, 40].

5.2. Germania

The role of tetrahedral rotation in GeO_2 α-quartz under pressure is considered to be less pronounced than in the silica equivalent, with angular distortion of the tetrahedra playing a more significant role [47]. Given that the apparently fortuitous combination of framework structure and applied loading direction along x_3 leads to deformation via concurrent rotation and dilation of the tetrahedra in SiO_2 (see above), it is interesting to pose the question as to whether or not this dual mechanism also acts in the GeO_2 structures under the same loading condition, or whether angular distortion of the tetrahedra is more likely to occur.

The fit of the CTM to the experimental ν_{31} value for GeO_2 α-quartz requires a value of $\kappa = 2.810$, corresponding to

a value of $\mathrm{d}\sec\theta/\mathrm{d}R = -4.013$ Å^{-1}. Assuming this value of $\mathrm{d}\sec\theta/\mathrm{d}R$ applies also to GeO_2 α-cristobalite, corresponding to $\kappa = 3.245$ for this polymorph, leads to a CTM model prediction of a near zero Poisson's ratio ($\nu_{31} = +0.007$). The CTM prediction for undeformed GeO_2 α-cristobalite is, therefore, for a ν_{31} value of opposite sign to the silica counterpart, although it is noted that the δ, κ combination for GeO_2 α-cristobalite is in the vicinity of the transition from non-auxetic to auxetic behaviour (figure 5).

The values of κ for the germania structures are lower than those for the silica counterparts, indicating rotation of the tetrahedra assumes a decreasing importance (i.e. $\mathrm{d}\delta$ decreases with respect to $\mathrm{d}l$ in equation (13)) in the dual-mode deformation mechanism for germania if the CTM is valid. This could indicate that the energy mis-match between the (low energy) rotation of linked tetrahedra about the common oxygen atom and the (higher energy) dilation of the tetrahedra through stretching of the intratetrahedral Ge–O bond is less pronounced in the germania structures than the equivalent processes in the silica structures. In which case, other intratetrahedral distortions, such as O–Ge–O angle variation, leading to angular distortion of the tetrahedra (as opposed to dilation which retains tetrahedron shape) may also become significant and thus decrease the validity of the CTM for germania. Experimental determination or detailed computer modelling simulations of the mechanical properties and structural evolution of germania under loading along x_3 are now required to test further the effect of composition on the validity of the CTM in the α-quartz and α-cristobalite frameworks.

The CTM-predicted strain-dependent trends for the germania polymorphs are similar to those for the silica counterparts (figure 6(b)), i.e. compression along x_3 leads to positive Poisson's ratio response whereas extension leads eventually to auxetic behaviour. The effect of changing composition from SiO_2 to GeO_2 is to raise the value of ν_{31} for any given applied strain, and to increase the strain at which the transition from positive to negative Poisson's ratio response occurs.

A σ_3-induced second phase for GeO_2 cristobalite is predicted from the CTM to be similar to that proposed for the silica counterpart, i.e. corresponding to a β-cristobalite structure having a tilt angle of $\delta \sim 0°$ (figure 7(c)). The CTM-predicted σ_3-induced second phase for GeO_2 quartz has a tilt angle of $\delta = 12.5°$ (figure 7(c)). We are not aware of any experimental evidence for the existence of a distinct second ('β') phase for GeO_2 quartz. The tilt angle of the second phase predicted in the CTM is sensitive to the value of κ employed in the model. For example, a value of $\kappa = 4.20$ leads to a second phase for GeO_2 quartz corresponding to a value of $\delta = 0°$ (figure 9). Interestingly, at a value of $\kappa = 2.006$ the two predicted phases of GeO_2 quartz become degenerate (same predicted value of tilt angle $\delta = 26.5°$—figure 9).

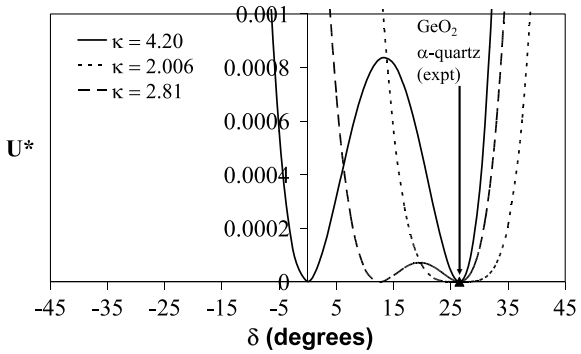

Figure 9. Normalized strain energy (U^*) versus tilt angle (δ) predictions from the CTM for GeO_2 quartz ($\delta_\alpha = 26.5°$): $\kappa = 4.20$ (solid line); $\kappa = 2.81$ (long dashed line); $\kappa = 2.006$ (short dashed line).

6. Conclusions

To conclude, simple analytical models have been developed in which the deformation of the α-quartz and α-cristobalite structures deform by rotation of the tetrahedra, dilation of the tetrahedra and concurrent rotation and dilation of the tetrahedra. The models have been applied to both silica and germania.

Tetrahedron rotation and tetrahedron dilation are both mechanisms giving rise to negative Poisson's ratios (auxetic behaviour), whereas both positive and negative values are possible when these mechanisms act concurrently. In particular, we have shown that concurrent rotation and dilation of the tetrahedra can explain both the positive and negative Poisson's ratios observed in SiO_2 α-quartz and SiO_2 α-cristobalite, respectively, when loaded in the x_3 direction. The remarkable accuracy with which the values are predicted by the model is attributable to the orientation of the tetrahedra with respect to this specific loading direction in these two polymorphs. Concurrent rotation and dilation of the tetrahedra leads to a positive ν_{31} to be predicted for both GeO_2 α-quartz and GeO_2 α-cristobalite. The predicted value for GeO_2 α-cristobalite is opposite in sign to that for the silica equivalent, although it is noted that the predicted value is very low (near zero) for GeO_2 α-cristobalite.

The strain-dependent ν_{31} trends due to concurrent rotation and dilation in the silica structures are in broad agreement with those predicted from pair-potential calculations, although significant differences do occur in the absolute values. It is likely that more degrees of freedom are required in the analytical models to reconcile the strain-dependent predictions with the pair-potential calculations, particularly at large strain where distortion of the tetrahedra may become a significant deformation mechanism. Predictions of the strain-dependent ν_{31} trends for the germania structures have been made, and the trends are similar to those for the silica structures. These now require verification through experimental measurement and alternative modelling methodologies.

The presence of a σ_3-induced second phase is predicted when deformation is due to rotation of the tetrahedra, or concurrent rotation and dilation of the tetrahedra. In the case of rotation of the tetrahedra the two phases correspond to equal but opposite signs of tilt angle, and so are likely to be energetically indistinguishable. Concurrent dilation and rotation of the tetrahedra, on the other hand, leads to two

clearly distinguishable phases having different values of tilt angle. The second phases predicted for silica are in reasonable agreement with the β- and idealized β-phases for quartz and cristobalite, respectively. The predicted second phase for SiO_2 cristobalite is also consistent with the ordered β-cristobalite structure, although an additional rotation system, not present in the current CTM model, is required to operate for this transformation to occur from the α-phase. The predicted second phase for GeO_2 cristobalite is also consistent with the idealized β-cristobalite structure.

In the absence of any experimental data, a model prediction for Poisson's ratio has been made for GeO_2 α-cristobalite. Experimental Poisson's ratio data for this germania polymorph are now required to test whether the CTM model is as applicable to germania as it has been found to be for silica [25].

References

[1] Evans J S O, Mary T A and Sleight A W 1997 *J. Solid State Chem.* **133** 580
[2] Veselago V 1968 *Sov. Phys.—Usp.* **10** 509
[3] Pendry J 2001 *Phys. World* **14** (9) 47
[4] Lakes R S 1987 *Science* **235** 1038
[5] Evans K E, Nkansah M A, Hutchinson I J and Rogers S C 1991 *Nature* **353** 124
[6] Baughman R H, Shacklette J M, Zakhidov A A and Stafstrom S 1998 *Nature* **392** 362
[7] Alderson K L, Pickles A P, Neale P J and Evans K E 1994 *Acta Metall. Mater.* **42** 2261
[8] Yeganeh-Haeri A, Weidner D J and Parise J B 1992 *Science* **257** 650
[9] Caddock B D and Evans K E 1989 *J. Phys. D: Appl. Phys.* **22** 1877
[10] Wei G and Edwards S F 1998 *Phys. Rev.* E **58** 6173
[11] Baughman R H and Galvao D S 1993 *Nature* **365** 735
[12] He C, Liu P and Griffin A C 1998 *Macromolecules* **31** 3145
[13] Evans K E, Alderson A and Christian F R 1995 *J. Chem. Soc. Faraday Trans.* **91** 2671
[14] Alderson A, Davies P J, Evans K E, Alderson K L and Grima J N 2005 *Mol. Simul.* **31** 889
[15] Alderson A 1999 *Chem. Ind.* 384
[16] Keskar N R and Chelikowsky J R 1992 *Nature* **358** 222
[17] Keskar N R and Chelikowsky J R 1993 *Phys. Rev.* B **48** 16227
[18] Grima J N, Jackson R, Alderson A and Evans K E 2000 *Adv. Mater.* **12** 1912
[19] Kimizuka H, Kaburaki H and Kogure Y 2000 *Phys. Rev. Lett.* **84** 5548
[20] Bowick M, Cacciuto A, Thorleifsson G and Travesset A 2001 *Phys. Rev. Lett.* **87** 148103
[21] O'Keeffe M and Hyde B G 1976 *Acta Crystallogr.* B **32** 2923
[22] Tautz F S, Heine V, Dove M T and Chen X 1991 *Phys. Chem. Minerals* **18** 326
[23] Alderson A and Evans K E 2001 *Phys. Chem. Minerals* **28** 711
[24] Megaw H D 1971 *Mater. Res. Bull.* **6** 1007
[25] Alderson A and Evans K E 2002 *Phys. Rev. Lett.* **89** 225503
[26] Grimsditch M, Polian A, Brazhkin V and Balitskii D 1998 *J. Appl. Phys.* **83** 3018
[27] Alderson K L, Alderson A and Evans K E 1997 *J. Strain Anal.* **32** 201
[28] Beatty M F and Stalnaker D O 1986 *J. Appl. Mech.* **53** 807
[29] McSkimin H J, Andreatch P Jr and Thurston R N 1965 *J. Appl. Phys.* **36** 1624
[30] Sevik C and Bulutay C 2007 *J. Mater. Sci.* **42** 6555
[31] Grimm H and Dorner B J 1975 *Phys. Chem. Solids* **36** 407
[32] Pluth J J, Smith J V and Faber J Jr 1985 *J. Appl. Phys.* **57** 1045
[33] Glinnemann J *et al* 1992 *Z. Kristallogr.* **198** 177
[34] Seifert K J, Nowotny H and Hanser E 1971 *Monatsh. Chem.* **102** 1006
[35] Jorgensen J D 1978 *J. Appl. Phys.* **49** 5473
[36] Schmahl W W, Swainson I P, Dove M T and Graeme-Barber A 1992 *Z. Kristallogr.* **201** 125
[37] Haines J, Cambon O, Philippot E, Chapon L and Hull S 2002 *J. Solid State Chem.* **166** 434
[38] Levien L, Prewitt C T and Weidner D J 1980 *Am. Mineral.* **65** 920
[39] Alderson A, Alderson K L, Evans K E, Grima J N, Williams M R and Davies P J 2004 *Comput. Methods Sci. Technol.* **10** 117
[40] Alderson A, Alderson K L, Evans K E, Grima J N, Williams M R and Davies P J 2005 *Phys. Status Solidi* b **242** 499
[41] Smirnov M B and Mirgorodsky A P 1997 *Phys. Rev. Lett.* **78** 2413
[42] Wyckoff R W G 1925 *Am. J. Sci.* **9** 448
[43] Leadbetter A J, Smith T W and Wright A F 1973 *Nature* **244** 125
[44] Wright A F and Leadbetter A J 1975 *Phil. Mag.* **31** 1391
[45] Nieuwenkamp W 1937 *Z. Kristallogr.* **96** 454
[46] Hatch D M and Ghose S 1991 *Phys. Chem. Mineral.* **17** 554
[47] Taylor D 1984 *Mineral. Mag.* **48** 65